Kinetics of Multistep Hole Transfer in DNA by Monitoring the Transient Absorption of the Pyrene Radical Cation

Tadao Takada, Kiyohiko Kawai, Sachiko Tojo, and Tetsuro Majima*

The Institute of Scientific and Industrial Research (SANKEN), Osaka University, Mihogaoka 8-1, Ibaraki, Osaka 567-0047, Japan

Received: June 20, 2003; In Final Form: September 9, 2003

To clarify the hole-transfer mechanism in DNA and the factor controlling the hole-transfer rates, the kinetics of hole transfer in DNA was studied by monitoring the transient absorption of the pyrene (Py) radical cation ($Py^{\bullet+}$) during the pulse radiolysis of oligodeoxynucleotides (ODNs) conjugated with Py. By analyzing the transient absorption of $Py^{\bullet+}$ formed by the hole transfer from DNA to Py, the rate constants of the hole transfer in various sequences of DNA were determined. The rate constants of the hole transfer from the nearest guanine (G) to Py were weakly dependent upon the distance between Py and the nearest G, indicating the occurrence of the multistep hole transfer in DNA. In contrast, in the hole transfer where the rate-determining step was the single-step hole transfer between Gs, the rate was strongly dependent upon the distance between the Gs. Comparing the intervening nucleobases between Gs, the rate constants of the multistep hole transfer increased in the order $G^{\bullet+}AG > G^{\bullet+}AC > G^{\bullet+}TG$. These results showed that the hole transfer between Gs was effectively mediated when the bridge was A. The effect of multiple Gs (GGG) on multistep hole transfer was examined. The hole transfer from DNA to Py was slowed by the presence of the GGG site that was far away from Py, indicating that the multiple G worked as a hole trap site. Our results are discussed in the context of the previously reported theoretical and experimental results.

Introduction

The possibility that the 1D array of the π-stacked base in DNA might serve as a medium for long-range charge migration was suggested over 30 years ago.[1] Recently, it has been demonstrated that a hole generated in DNA can migrate over the long distance of 200 Å.[2,3] In most of the recent experimental studies, a hole (or electron) donor and acceptor are covalently attached to a DNA oligonucleotide with a well-defined base pair sequence.[4] The efficiency of the hole transport from the donor to the acceptor is then determined either by measuring the quenching of the donor fluorescence[4,5] or by an analysis of the relative yield of strand breakage at different positions along the DNA strand.[6] An understanding of the oxidative damage of the double-helical DNA and the design of DNA-based devices for molecular devices is crucially dependent upon the elucidation of the mechanism and kinetics of electron and hole transport in DNA;[6,7] therefore, the factor controlling the hole-transfer rates have been extensively studied.[8]

DNA oxidative damage in these studies is quantified by measuring strand breaks after piperidine treatment of 5′-^{32}P-end-labeled DNA and gel electrophoresis.[2] A mixture of tunneling and hopping mechanisms has been proposed. The most widely accepted model is a multistep hole-hopping mechanism in which a hole migrates via a random walk between sites localized on G, GG, and GGG.[9,10] In addition, DNA hole transfer has been demonstrated to occur by two different mechanisms: G hopping (superexchange between Gs across the intervening A-T bridge) and A hopping (the hole is carried by the bridge base A as $A^{\bullet+}$).[11] An alternative mechanism in which a delocalized hole migrates via a polaronlike hopping mechanism has been suggested by Schuster.[3,12,13] Barton and co-workers have proposed that the hole transfer through DNA depends on the conformational dynamics of the DNA associated with these sequences.[14]

There are many reports of the direct measurements of the kinetics of hole transfer between the hole donor and acceptor separated by nucleobases in DNA. Lewis et al. demonstrated the hole-transfer kinetics on the basis of femtosecond time-resolved transient absorption spectroscopy in hairpin DNA possessing stilbene as a linker.[4,15,16] Shafirovich et al. investigated the distance dependence of hole transfer from the 2-aminoprine radical cation to guanine separated by variable numbers of thymine or adenine bases on the microsecond time scale during the two-photon ionization monitored by transient absorption.[17]

Hole-injection efficiency during the photoinduced electron transfer from a photosensitizer to a neighbor nucleobase is low because of the contribution of rapid charge recombination.[18] Therefore, it is difficult to observe the multistep hole-transfer process by the transient absorption measurement. We have previously reported the observation of the hole-transfer process on the basis of the pulse radiolysis method[19,20] and have demonstrated that hole transfer through DNA occurred on a time scale of 100 μs.[20,21] Pulse radiolysis is advantageous to the generation of radical ions, and a hole can be generated in DNA up to 10^{-5} M during pulse radiolysis. Furthermore, to detect the hole-transfer process, oligodeoxynucleotides (ODNs) conjugated with a probe molecule, pyrene (Py), of which the radical cation ($Py^{\bullet+}$) has a distinct absorption spectrum with a maximum at 470 nm, was synthesized. By monitoring the transient absorption of $Py^{\bullet+}$ formed by the hole transfer from ODN to Py, the single- and multistep hole-transfer processes were investigated. We now describe the kinetics of the multistep hole

* Corresponding author. E-mail: majima@sanken.osaka-u.ac.jp.

10.1021/jp035750k CCC: $25.00
Published on Web 11/21/2003

transfer from the G region in ODN to Py, the distance dependence of the hole transfer from the primary G to the secondary G, interstrand and intrastrand hole transfer, and the influence of multiple G as a hole trap. The obtained results are in good agreement with the previously reported theoretical and experimental results.

Experimental Section

Oligodeoxynucleotides (ODNs). The ODNs were synthesized using an Applied Biosystems DNA synthesizer with standard solid-phase techniques and purified on a JASCO HPLC with a reverse-phase C-18 column and an acetonitrile/50 mM ammonium formate gradient. Duplex solutions (20 mM sodium phosphate buffer, pH 7) were prepared by mixing equimolar amounts of the desired ODN complements and gradually annealing with cooling from 80 °C to room temperature. The ODNs conjugated with pyrene at a terminal site were synthesized by the automated solid-phase phosphoramidite method according to a previous report[22] and were then purified by HPLC as mentioned above. The purity and concentration of all of the synthetic ODNs were determined by complete digestion with s.v. PDE, P1 nuclease, and alkaline phosphatase to 2′-deoxymononucleosides.

Measurements of Melting Temperature. Thermal denaturation profiles were obtained using a JASCO V-530 spectrophotometer equipped with a Peltier temperature controller. The absorbance of the ODN sample (4 μM duplex in 20 mM phosphate buffer (pH 7.0)) was monitored at 260 nm (A_{260}) from 10 to 70 °C at a heating rate of 1 °C min^{-1}. The melting temperature (T_m) was determined as the maximum in a plot of $\Delta A_{260}/\Delta T$ versus T.

Pulse Radiolysis. A hole in DNA was generated from the one-electron oxidation by $SO_4^{\bullet-}$ during pulse radiolysis using an electron pulse (28 MeV, 8 ns, 0.7 kGy pulse^{-1}) of an Ar-saturated aqueous solution containing 10 mM $S_2O_8^{2-}$, 100 mM *t*-BuOH, 20 mM Na phosphate buffer (pH 7.0), and 0.05−0.2 mM ODN at 23 °C. A xenon flash lamp (Osram, XBO-450), which was synchronized with the electron pulse, was focused through the sample as a probe light for the transient absorption measurement. The time profiles of the transient absorption were measured with a monochromator (CVI, DK-240) equipped with a photomultiplier (Hamamatsu Photonics, R928) and a digital oscilloscope (Tektronix, TDS 580D). For the time-resolved transient absorption spectral measurement, the monitor light was focused into a quartz optical fiber, which transported the light to a gated multichannel spectrometer (Unisoku, TSP-601-02).

Results and Discussion

Synthesis and Melting-Temperature Measurements for ODN Conjugated with Pyrene. Oligodeoxynucleotides (ODNs) conjugated with pyrene (Py) at a terminal site were synthesized by the automated solid-phase phosphoramidite method according to a previous report.[22] The ODN designed for the investigation of the hole-transfer kinetics are shown in Chart 1. ODNs Py-G*n* (*n* means the number of AT base pairs between Py and the nearest G) were designed to examine the multistep hole transfer between Gs. ODNs G-G*n* were synthesized in terms of the single-step hole transfer between Gs because the rate-determining step was expected for the hole transfer between the primary G and secondary G. ODNs Py-ACAC, AGAG, ACAG, and AGAC were designed to investigate the intra- versus interstrand hole transfers and the effect of intervening nucleobases between Gs. ODNs Py-GGG*n* (*n* represents GGG in the ODN strand)

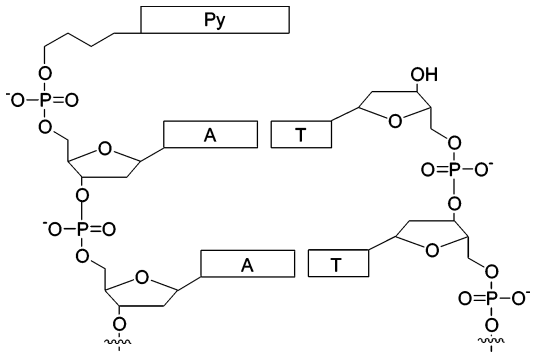

Figure 1. Schematic representation of π stacking of the 5′-end-labeled pyrene on the neighboring A-T base pair.

CHART 1: Sequences of ODNs Used in This Study

(A) Py-Gn(n=1-5)

Py−(A/T)$_n$−CACACAC−(A/T)$_{6-n}$
(A/T)$_n$−GTGTGTG−(A/T)$_{6-n}$

(B) G-Gn(n=1-4)

Py − AC −(A/T)$_n$−CGCGC −(A/T)$_{5-n}$
TG −(A/T)$_n$−GCGCG −(A/T)$_{5-n}$

(C) Intra- and inter-strand hole transfer

Py-ACAC
Py-ACACACACACA
TGTGTGTGTGT

Py-AGAG
Py-AGAGAGAGAGA
TCTCTCTCTCT

Py-ACAG
Py-ACAGACAGACA
TGTCTGTCTGT

Py-AGAC
Py-AGACAGACAGA
TCTGTCTGTCT

(D) Py-GGGn(n=1-4)

Py − A −(CA/GT)$_{n-1}$−CCCA −(CA/GT)$_{4-n}$
T −(CA/GT)$_{n-1}$−GGGT −(CA/GT)$_{4-n}$

Py was covalently attached at the 5′-end.

were designed to examine the influence of multiple G species as a hole trap on the hole-transfer process.

Because Py has a planar structure and is hydrophobic, π stacking between the 5′-end-labeled Py and neighboring nucleobases is expected (Figure 1). Melting-temperature profiles for Py-Gn = 1 and Gn = 1 are shown in Figure 2. Increasing the T_m value for ODN conjugated with Py (T_m = 39.1 °C) compared to the unmodified ODN (T_m = 34.2 °C) indicates the stabilization of ODN due to the end capping of Py with nucleobases. Similar stabilization by end capping has been observed for DNA conjugated with anthraquinone.[12]

One-Electron Oxidation of DNA by Oxidant $SO_4^{\bullet-}$ during Pulse Radiolysis. The hydrated electron (e_{aq}^-) generated during the pulse radiolysis of water with an electron pulse (8 ns, 28 MeV) reacts with $S_2O_8^{2-}$ to produce the strong oxidant $SO_4^{\bullet-}$ ($E°$ = 2.5−3.1 V vs NHE in H_2O), which is powerful enough to oxidize all four DNA bases.[23,24] The efficient number of holes in ODN was generated from the one-electron oxidation of ODN by $SO_4^{\bullet-}$ during pulse radiolysis as shown by path a of Figure 3. The hole transfer from G to Py is expected to occur because the oxidation potential of Py ($E°$ = 1.40 V vs NHE in CH_3CN) is lower than that of G ($E°$ = 1.47 V vs NHE in CH_3CN), which is the most easily oxidizable base among the four DNA bases (Figure 3, path b).[21] The hole-transfer process from ODN to Py and the expected rate-determining step are shown in Figure 4, and the kinetics of the sequence dependence of multistep

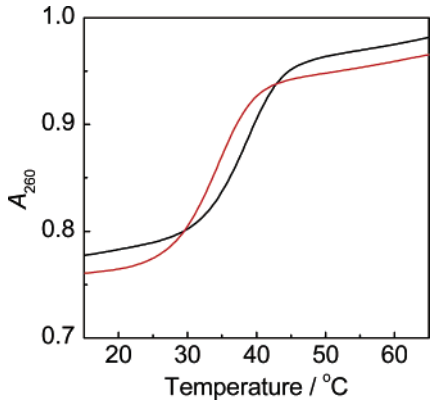

Figure 2. Melting-temperature profiles for Py-G*n* ($n = 1$) (black) and G*n* ($n = 1$) (unconjugated with pyrene, red). The melting behavior was determined in an aqueous solution containing 4 μM duplex (strand conc) and 20 mM Na phosphate buffer (pH 7.0) from the absorbance at 260 nm (A_{260}).

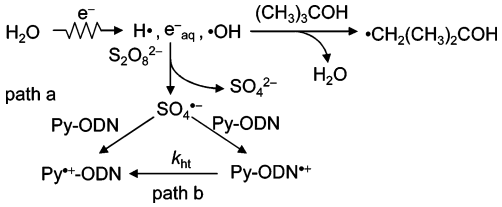

Figure 3. Scheme of the one-electron oxidation of ODN after irradiation with an electron pulse during the pulse radiolysis of an Ar-saturated aqueous solution containing 0.2 mM ODN, 10 mM $K_2S_2O_8$, 100 mM *t*-BuOH, and 20 mM Na phosphate buffer (pH 7.0).

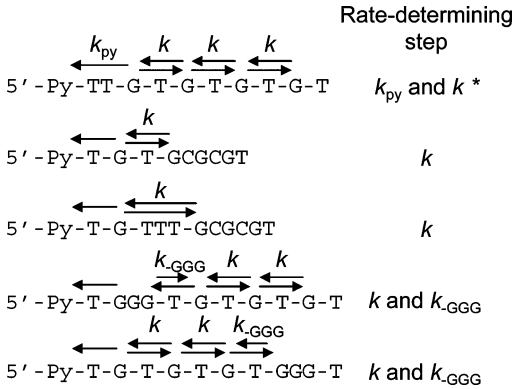

Figure 4. Schematic illustration of the hole-transfer process from ODN to Py and the expected rate-determining step for each system. The rate-determining step, indicated with an asterisk, is dependent on the number of A-T base pairs between Py and the nearest G.

hole transfer was studied by analyzing the formation of the Py radical cation.

Transient absorption spectra with a maximum peak at 470 nm assigned to $Py^{\bullet+}$ were observed after the irradiation of an electron pulse during pulse radiolysis (Figure 5). No occurrence of the decay of $Py^{\bullet+}$ on the time scale of 100 μs indicates that the oxidation potential of Py is lower than that of G. The formation rates of $Py^{\bullet+}$ within several microseconds were linearly dependent on the concentration of the Py-conjugated ODN (0.05−0.2 mM), indicating the formation of $Py^{\bullet+}$ from the direct diffusional collision between the Py site and the $SO_4^{\bullet-}$ oxidant (Figure 3, path a). The rate constants of the one-electron oxidation of the Py site by $SO_4^{\bullet-}$ were determined by analyzing the formation rate of $Py^{\bullet+}$, which is dependent on the concentration of ODN, and the rate constants for ODN unconjugated with Py were determined by monitoring the formation of $G^{\bullet+}$ (or deprotonated $G^{\bullet}(-H^+)$) at 400 nm.[23] These values are shown in Table 1. The rate constants for the Py-conjugated and unconjugated ODN were similar, indicating the competitive oxidation of the Py and ODN sites by $SO_4^{\bullet-}$.

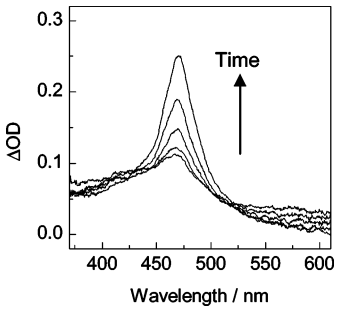

Figure 5. Transient absorption spectra monitored for Py-G*n* ($n = 1$) at 100, 200, and 500 ns and 1 and 10 μs after the irradiation of an electron pulse during the pulse radiolysis of an Ar-saturated aqueous solution containing 0.2 mM ODN, 10 mM $K_2S_2O_8$, 100 mM *t*-BuOH, and 20 mM Na phosphate buffer (pH 7.0).

TABLE 1: Rate Constants of One-Electron Oxidation for Py-ODN and Unmodified ODN by Oxidant $SO_4^{\bullet-}$ during Pulse Radiolysis

ODN	k_{Py-ODN}[a]/ 10^9 M^{-1} s^{-1}	k_{ODN}[a]/ 10^9 M^{-1} s^{-1}
Py-G*n* ($n = 1$)	4.4	2.8
Py-G*n* ($n = 5$)	4.5	3.3

[a] Rate constants of one-electron oxidation for ODN conjugated and unconjugated with Py were determined by monitoring the formation of the transient absorption of $Py^{\bullet+}$ at 470 nm and $G^{\bullet+}$ (or deprotonated $G^{\bullet}(-H^+)$) at 400 nm, respectively.

Distance Dependence of the Hole Transfer from the G Region to Pyrene. The ODNs of Py-G*n* ($n = 1-5$) were designed to examine the hole-transfer kinetics depending on the distance between Py and the nearest G (Chart 1A). Time profiles of the transient absorption of $Py^{\bullet+}$ monitored at 470 nm for Py-G*n* ($n = 1-5$) are shown in Figure 6. In all of the Py-G*n*'s ($n = 1-5$), the initial direct oxidation of the Py site by $SO_4^{\bullet-}$ was completed in 2 μs. After the completion of the initial collisional process, that is, the consumption of $SO_4^{\bullet-}$ and the formation of $Py^{\bullet+}$ and $G^{\bullet+}$, the secondary formation of $Py^{\bullet+}$ was clearly observed in the case of Py-G*n* ($n = 1, 2$). This was attributed to the hole transfer from the G region to the Py site.

Because the hole transfer from the G region to the Py site is considered to be much slower for Py-G*n* ($n = 5$) compared to that for Py-G*n* ($n = 1-4$), $Py^{\bullet+}$ for Py-G*n* ($n = 5$) was formed only from the initial direct oxidation by $SO_4^{\bullet-}$. The time profile of $Py^{\bullet+}$ for Py-G*n* ($n = 5$) was subtracted from those for Py-G*n* ($n = 1-4$). This suggested the formation of $Py^{\bullet+}$ from the hole transfer in DNA, demonstrating that the hole transfer in DNA occurred on the time scale of ~100 μs. The rate constants of the hole transfer for Py-G*n* ($n = 1-4$) were determined from fitting the time profile with a single exponential (Table 2). The rate constant decreased with the increase in the distance between Py and the G region.

In the case of Py-G*n*, the rate-determining step in the multistep hole-transfer process is dependent upon the number of A-T base pairs between Py and the nearest G. Unfortunately, we could not determine the rate-determining step in the sequence of Py-G*n*. Therefore, the observed rate constants of hole transfer were described by the rate constants containing the hole-transfer process from the nearest G to Py (k_{py}) and between G bases (k) as shown in Figure 4. When the natural logarithms of the hole-transfer rate ($\ln k_{ht}$) were plotted against Δr, a linear relationship

TABLE 2: Sequence of ODN Conjugated with Pyrene (Py) and the Rate Constants of Hole Transfer from ODN to Py

ODN	sequence[a]	k_{ht}[b,c]/ 10^4 s^{-1}	ODN	sequence[a]	k_{ht}[b,c]/ 10^4 s^{-1}
Py-G*n* (*n* = 1)	Py-ACACACACAAAAA	11	Py-ACAC	Py-ACACACACACA	6.3
Py-G*n* (*n* = 2)	Py-AACACACACAAAA	6.7	Py-AGAG	Py-AGAGAGAGAGA	>100
Py-G*n* (*n* = 3)	Py-AAACACACACAAA	2.1	Py-ACAG	Py-ACAGACAGACA	14
Py-G*n* (*n* = 4)	Py-AAAACACACACAA	0.8	Py-AGAC	Py-AGACAGACAGA	20
Py-G*n* (*n* = 5)	Py-AAAAACACACACA		Py-GGG1	Py-ACCCACACACA	16
G-G*n* (*n* = 1)	Py-ACACGCGCAAAA	2.8	Py-GGG2	Py-ACACCCACACA	3.9
G-G*n* (*n* = 2)	Py-ACAACGCGCAAA	0.3	Py-GGG3	Py-ACACACCCACA	1.3
G-G*n* (*n* = 3)	Py-ACAAACGCGCAA	<0.1	Py-GGG4	Py-ACACACACCCA	1.6
G-G*n* (*n* = 4)	Py-ACAAAACGCGCA				

[a] Represents the sequence of ODN modified with Py. [b] See text for detail. [c] Estimated error of the reported value of the rate constants was ±20%.

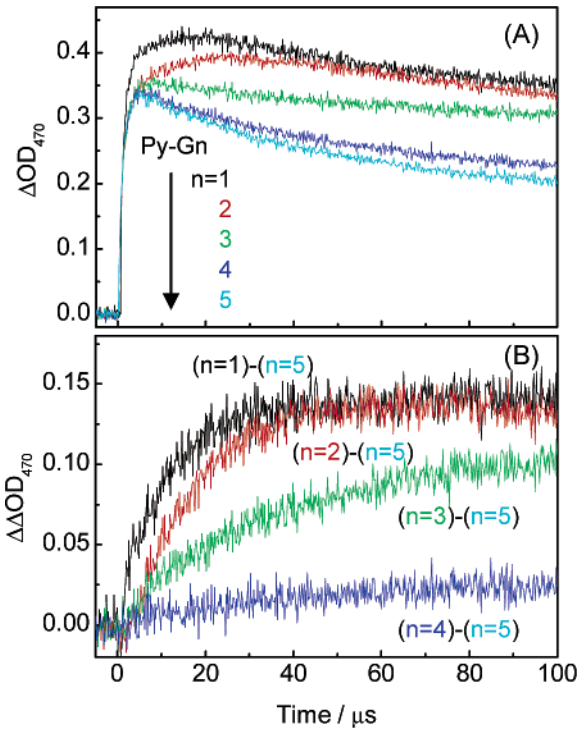

Figure 6. Time profiles of the transient absorption of Py$^{\bullet+}$ monitored at 470 nm for (A) Py-G*n* (*n* = 1−5) and (B) Py-G*n* (*n* = 1−4) after subtracting the time profile for Py-G*n* (*n* = 5).

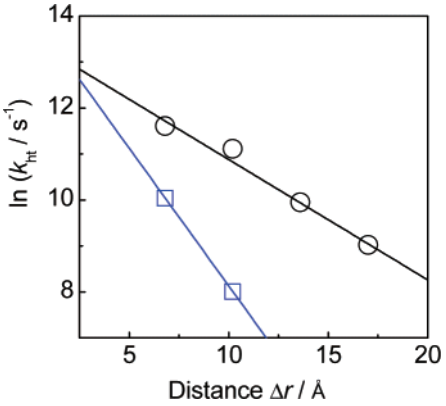

Figure 7. Distance dependence of the hole-transfer rates for Py-G*n* (black circles and line) and G-G*n* (blue squares and line). log(k_{ht}) was plotted against the distance (Δr) between Py and the nearest G for Py-G*n* and between the primary G and the secondary G for G-G*n*. Values of Δr were calculated assuming an average distance of 3.4 Å between bases.

was observed (Figure 7). From the slope of the linear plot, a value of 0.3 ± 0.03 Å^{-1} was obtained for the distance dependence of the hole transfer from the G region to Py. This smaller value of 0.3 ± 0.03 Å^{-1} compared to the reported β value (0.6−1.3 Å^{-1}) [4,16,17] obtained in the photoinduced electron transfer must result from the weak distance-dependent hole-transfer process. Therefore, the multistep hole-transfer processes between Gs in the G region can be assumed to occur. Considering that the rate constant of the hole transfer from the first G to the second G through one AT base pair (GTG) reported by Lewis[16] is 2 × 10^5 s^{-1} and that the hole transfer from the G region to Py is a multistep process, the obtained values of k_{ht} are considered to be appropriate.

Effects of the Number of AT Base Pairs between two Gs. The ODNs (G-G*n* (*n* = 1−4)) that possess the primary G separated from the secondary G by several AT base pairs were designed to investigate the effect of the distance between Gs on the hole transfer (Chart 1B). The rate-determining step of the hole-transfer process from ODN to Py is expected to be hole transfer between the primary G and secondary G because the hole transfer from the primary G to Py is exergonic and other Gs are in contact with the next G (Figure 4).

The time profiles of the transient absorption of Py$^{\bullet+}$ monitored at 470 nm observed after the electron pulse during the pulse radiolysis are shown in Figure 8. The time profiles for G-G*n* (*n* = 3, 4) were similar, indicating that the hole transfer did not occur on this time scale, whereas the time profiles for G-G*n* (*n* = 1, 2) were different from those for G-G*n* (*n* = 3, 4)(Figure 8A). As mentioned above, the rate constants for the multistep hole transfer were obtained by subtracting the time profile for G-G*n* (*n* = 4) from that for G-G*n* (*n* = 1, 2) (Figure 8B and Table 2). The rate constants decreased with an increase in the number of AT base pairs by a factor of 10, and the slope of the two rate constants for G-G*n* (*n* = 1, 2) was 0.6 ± 0.1 Å^{-1} (Figure 5), which is similar to the previously reported β value in the photoinduced electron transfer and hole transfer in DNA.[16] These results suggest that the determining step is the hole transfer that occurs from the primary G to the secondary G via a superexchange mechanism.[9,16] The difference between the value of 0.3 Å^{-1} for Py-G*n* and the β value of 0.6 Å^{-1} for G-G*n* might be attributed to the different hole-transfer mechanisms, that is, the multistep hole-transfer mechanism in the GTGTGTG sequence for Py-G*n* and the single-step hole-transfer mechanism in the G-A$_n$-G sequence for G-G*n*.

Interstrand versus Intrastrand Hole Transfer. To elucidate the inter- and intrastrand hole-transfer kinetics, the formation and decay of Py$^{\bullet+}$ during the pulse radiolysis were investigated for ODNs that possess the AGAG, TGTG, ACAG, and AGAC repeat sequences as mentioned above (Chart 1C, Figure 9). With respect to the intrastrand sequences (Py-AGAG, Py-ACAC) in which the Gs were separated by A bases on the same strand, the rate constant of the hole transfer for Py-AGAG increased

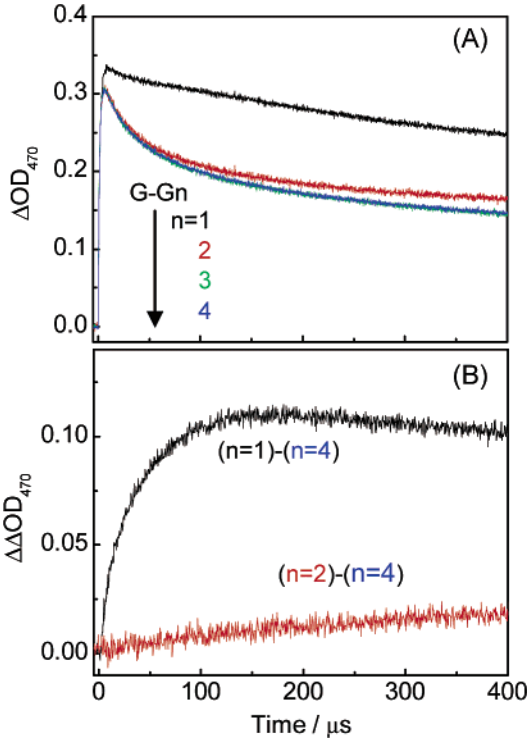

Figure 8. Time profiles of the transient absorption of $Py^{\bullet+}$ monitored at 470 nm for (A) G-G*n* ($n = 1-4$) and (B) G-G*n* ($n = 1, 2$) after subtracting the time profile of G-G*n* ($n = 4$).

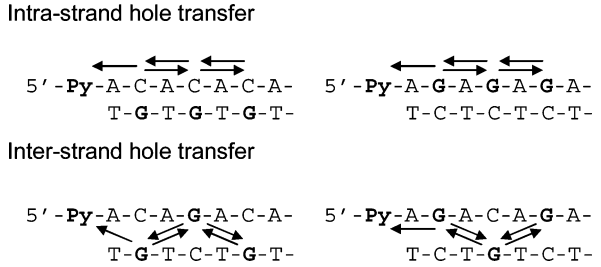

Figure 9. Schematic illustration of intra- and interstrand hole transfer.

by a factor of 15 compared to that for Py-ACAC (Table 2). This result indicates that the hole transfer from G to G on the same strand was influenced by the stacking of A with G. For the interstrand sequences (Py-ACAG, Py-AGAC), the rate constants of the hole transfer for Py-ACAG and Py-AGAC were similar but larger than that for Py-ACAC. This difference is attributed to the stacking of one of the Gs with A. On the basis of these results, the rate constants for the hole transfer between Gs were in the order $G^{\bullet+}AG > G^{\bullet+}AC > G^{\bullet+}TG$. This order is in agreement with that for the single-step hole transfer from the primary G to the secondary G reported by Lewis et al.[16] Considering that the oxidation potential of A is higher than that of G but lower than those of C and T,[23,25] the hole transfer is accelerated by lowering the ionization potential of the bridged bases between Gs. Previously, it has been experimentally and theoretically shown that lowering the ionization potential of a bridge increases the electronic coupling for the superexchange interaction and influences the tunneling energy.[26]

Influence of Multiple Gs (GGG) as a Hole Trap on the Hole-Transfer Process. ODNs Py-GGG*n* ($n = 1-4$), in which GGG sites were located at a different site than Py, were designed to examine the influence of GGG as the hole trap on the hole-transfer kinetics (Chart 1D). Strand-cleavage reactions, induced by piperidine treatment following oxidative damage, have consistently shown that multiple Gs in DNA are more susceptible to oxidative damage than isolated Gs.[9,27] This feature has been utilized in long-range hole-transfer studies, which are based on GGG being a better trap than a single G base. These results were explained by the stacking effect of consecutive Gs, which lowered the ionization potential.[28] The rate constants for the hole transfer from ODN to Py were determined according to the procedure mentioned above and are shown in Table 2. These values showed that the rate constants of the hole transfer decreased with an increase in the distance between Py and GGG, indicating that the GGG site worked as the hole trap and slowed the hole transfer to Py. A hole generated in Py-GGG*n* ($n = 1-4$) finally migrated to Py, suggesting the existence of a hole equilibrium between the single G and multiple Gs (GGG) at room temperature. From the kinetic studies using the transient absorption measurements, Lewis and co-workers have demonstrated the difference in thermodynamic stability (ΔG) at consecutive Gs; the ΔG values of GG and GGG versus G are -52 and 77 meV, respectively.[29] A similar stacking effect on the ionization potential has been calculated by Kurnikov et al.[30] Our results are in agreement with these results and showed that although shallow GGG served as a hole trap.

Conclusions

We have demonstrated hole-transfer kinetics by monitoring the transient absorption of $Py^{\bullet+}$ during pulse radiolysis, (i) the multistep hole transfer from the G region to Py, (ii) the distance dependence of the hole transfer from the primary G to the secondary G, (iii) interstrand and intrastrand hole transfer, and (iv) the influence of multiple Gs as a hole trap. First, when Py conjugated to ODN at a terminal site was separated from the nearest G by several AT base pairs, the rate constants of the hole transfer decreased with an increase in the distance but was weakly dependent on the distance, indicating the occurrence of the multistep process. Second, from the analysis of the linear plot of ln k_{ht} against the distance between Gs for G-G*n*, it was shown that the single-step hole transfer from the primary G to the secondary G was strongly dependent on the distance. Third, for the intra- and interstrand hole-transfer kinetics, the apparent rate constants of the hole transfer were in the order $G^{\bullet+}TG < G^{\bullet+}AC < G^{\bullet+}AG$. Therefore, A is found to be a better medium than T. This difference could be attributed to the lower oxidation potential of A than that of T and the direct stacking of G with A. Finally, the GGG site worked as the shallow hole trap, and hole equilibrium existed between G and GGG. Our results provide valuable information about the kinetics of the single- and multistep hole transfer and indicated that the hole transfer in DNA occurred on a microsecond time scale and was dependent upon the DNA sequences and intervening nucleobases between Gs.

Acknowledgment. We thank the members of the Radiation Laboratory of ISIR, Osaka University for running the linear accelerator. This work has been partially supported by a Grant-in-Aid for Scientific Research on Priority Area (417) and others from the Ministry of Education, Culture, Sports and Science, and Technology (MEXT) of the Japanese Government.

References and Notes

(1) Eley, D. D.; Spivey, D. I. *Trans. Faraday Soc.* **1962**, *58*, 411−415.

(2) Nunez, M. E.; Hall, D. B.; Barton, J. K. *Chem. Biol.* **1999**, *6*, 85−97.

(3) Henderson, P. T.; Jones, D.; Hampikian, G.; Kan, Y. Z.; Schuster, G. B. *Proc. Natl. Acad. Sci. U.S.A.* **1999**, *96*, 8353−8358.

(4) Lewis, F. D.; Letsinger, R. L.; Wasielewski, M. R. *Acc. Chem. Res.* **2001**, *34*, 159−170.

(5) (a) Kelley, S. O.; Barton, J. K. *Science* **1999**, *283*, 375−381. (b) Fukui, K.; Tanaka, K. *Angew. Chem., Int. Ed.* **1998**, *37*, 158−161. (c) Wan, C. Z.; Fiebig, T.; Schiemann, O.; Barton, J. K.; Zewail, A. H. *Proc. Natl. Acad. Sci. U.S.A.* **2000**, *97*, 14052−14055.

(6) Burrows, C. J.; Muller, J. G. *Chem. Rev.* **1998**, *98*, 1109−1151.

(7) (a) Armitage, B. *Chem. Rev.* **1998**, *98*, 1171−1200. (b) Boon, E. M.; Salas, J. E.; Barton, J. K. *Nat. Biotech.* **2002**, *20*, 282−286. (c) Porath, D.; Bezryadin, A.; de Vries, S.; Dekker, C. *Nature* **2000**, *403*, 635−638.

(8) (a) Bixon, M.; Jortner, J. *J. Am. Chem. Soc.* **2001**, *123*, 12556−12567. (b) Conwell, E. M.; Basko, D. M. *J. Am. Chem. Soc.* **2001**, *123*, 11441−11445. (c) Voityuk, A. A.; Jortner, J.; Bixon, M.; Rosch, N. *Chem. Phys. Lett.* **2000**, *324*, 430−434.

(9) Meggers, E.; Michel-Beyerle, M. E.; Giese, B. *J. Am. Chem. Soc.* **1998**, *120*, 12950−12955.

(10) (a) Nakatani, K.; Dohno, C.; Saito, I. *J. Am. Chem. Soc.* **1999**, *121*, 10854−10855. (b) Giese, B.; Biland, A. *Chem. Commun.* **2002**, 667−672.

(11) (a) Giese, B.; Amaudrut, J.; Kohler, A. K.; Spormann, M.; Wessely, S. *Nature* **2001**, *412*, 318−320. (b) Kendrick, T.; Giese, B. *Chem. Commun.* **2002**, 2016−2017. (c) Kawai, K.; Takada, T.; Tojo, S.; Majima, T. *J. Am. Chem. Soc.* **2003**, *125*, 6842−6843.

(12) Schuster, G. B. *Acc. Chem. Res.* **2000**, *33*, 253−260.

(13) Barnett, R. N.; Cleveland, C. L.; Joy, A.; Landman, U.; Schuster, G. B. *Science* **2001**, *294*, 567−571.

(14) O'Neill, M. A.; Barton, J. K. *J. Am. Chem. Soc.* **2002**, *124*, 13053−13066.

(15) (a) Lewis, F. D.; Wu, T. F.; Zhang, Y. F.; Letsinger, R. L.; Greenfield, S. R.; Wasielewski, M. R. *Science* **1997**, *277*, 673−676. (b) Lewis, F. D.; Liu, J.; Liu, X.; Zuo, X.; Hayes, R. T.; Wasielewski, M. R. *Angew. Chem., Int. Ed.* **2002**, *41*, 1026−1028.

(16) Lewis, F. D.; Liu, J.; Zuo, X.; Hayes, R. T.; Wasielewski, M. R. *J. Am. Chem. Soc.* **2003**, *125*, 4850−4861.

(17) Shafirovich, V.; Cadet, J.; Gasparutto, D.; Dourandin, A.; Huang, W. D.; Geacintov, N. E. *J. Phys. Chem. B* **2001**, *105*, 586−592.

(18) (a) Lewis, F. D.; Liu, X. Y.; Liu, J. Q.; Miller, S. E.; Hayes, R. T.; Wasielewski, M. R. *Nature* **2000**, *406*, 51−53. (b) Lewis, F. D.; Wu, T. F.; Liu, X. Y.; Letsinger, R. L.; Greenfield, S. R.; Miller, S. E.; Wasielewski, M. R. *J. Am. Chem. Soc.* **2000**, *122*, 2889−2902.

(19) (a) Takada, T.; Kawai, K.; Tojo, S.; Majima, T. *Tetrahedron Lett.* **2003**, *44*, 3851−3854. (b) Kawai, K.; Takada, T.; Tojo, S.; Majima, T. *Tetrahedron Lett.* **2002**, *43*, 8083−8085.

(20) Kawai, K.; Takada, T.; Tojo, S.; Majima, T. *Tetrahedron Lett.* **2002**, *43*, 89−91.

(21) Kawai, K.; Takada, T.; Tojo, S.; Ichinose, N.; Majima, T. *J. Am. Chem. Soc.* **2001**, *123*, 12688−12689.

(22) Mann, J. S.; Shibata, Y.; Meehan, T. *Bioconjugate Chem.* **1992**, *3*, 554−558.

(23) Steenken, S.; Jovanovic, S. V. *J. Am. Chem. Soc.* **1997**, *119*, 617−618.

(24) (a) Candeias, L. P.; Steenken, S. *J. Am. Chem. Soc.* **1993**, *115*, 2437−2440. (b) Steenken, S. *Chem. Rev.* **1989**, *89*, 503−520.

(25) Seidel, C. A. M.; Schulz, A.; Sauer, M. H. M. *J. Phys. Chem.* **1996**, *100*, 5541−5553.

(26) (a) Nakatani, K.; Dohno, C.; Saito, I. *J. Am. Chem. Soc.* **2000**, *122*, 5893−5894. (b) Lewis, F. D.; Liu, J. Q.; Weigel, W.; Rettig, W.; Kurnikov, I. V.; Beratan, D. N. *Proc. Natl. Acad. Sci. U.S.A.* **2002**, *99*, 12536−12541. (c) Beratan, D. N.; Priyadarshy, S.; Risser, S. M. *Chem. Biol.* **1997**, *4*, 3−8. (d) Bixon, M.; Giese, B.; Wessely, S.; Langenbacher, T.; Michel-Beyerle, M. E.; Jortner, J. *Proc. Natl. Acad. Sci. U.S.A.* **1999**, *96*, 11713−11716.

(27) (a) Hickerson, R. P.; Prat, F.; Muller, J. G.; Foote, C. S.; Burrows, C. J. *J. Am. Chem. Soc.* **1999**, *121*, 9423−9428. (b) Saito, I.; Nakamura, T.; Nakatani, K.; Yoshioka, Y.; Yamaguchi, K.; Sugiyama, H. *J. Am. Chem. Soc.* **1998**, *120*, 12686−12687.

(28) Sugiyama, H.; Saito, I. *J. Am. Chem. Soc.* **1996**, *118*, 7063−7068.

(29) Lewis, F. D.; Liu, X. Y.; Liu, J. Q.; Hayes, R. T.; Wasielewski, M. R. *J. Am. Chem. Soc.* **2000**, *122*, 12037−12038.

(30) Kurnikov, I. V.; Tong, G. S. M.; Madrid, M.; Beratan, D. N. *J. Phys. Chem. B* **2002**, *106*, 7−10.